The Planetary Science Journal, 2:31 (10pp), 2021 February https://doi.org/10.3847/PSJ/abd403

Surfaces of (Nearly) Dormant Comets and the Recent History of the Quadrantid Meteor Shower

Theodore Kareta, Carl Hergenrother, Vishnu Reddy, and Walter M. Harris
Lunar and Planetary Laboratory, University of Arizona 1629 E University Avenue, Tucson, AZ, USA; tkareta@lpl.arizona.edu
Received 2020 September 23; revised 2020 December 13; accepted 2020 December 14; published 2021 February 22

Abstract

The parent of the Quadrantid meteor shower is the inactive solar system small body (196256) 2003 EH_1. EH_1 has likely only gone dormant in the past few hundred years, and may be related to the bright comet C/1490 Y1. Compared with the other best-studied inactive meteor shower parent (3200) Phaethon, EH_1 has received comparatively minimal characterization of its surface properties. We present the first reflectance spectrum and additional photometry of EH_1, as well as new spectra of the nuclei of three nearly dormant comets P/2006 HR_{30} (Siding Spring), 364P/Pan-STARRS, and 249P/LINEAR for comparison. We also present new short-term high-resolution orbital integrations of these bodies for context. EH_1s spectrum is red in color below 0.8 μm in between C and D types, consistent with previous photometric measurements, but is blue beyond 0.8 μm until at least 1.02 μm. 249P and 364P have both red slopes consistent with C taxonomic types and HR_{30} has a classic comet nucleus D-type slope. If the downturn in EH_1's spectrum is due to an absorption feature, magnetite and olivine are plausible candidates, but more data are needed. 249P and 364P have similar recent and historical dynamical evolutions in addition to their similar surface properties. We discuss the interrelation between the dynamical histories and modern surfaces of these four objects and suggest avenues for further study to better constrain how the Quadrantids and Geminids were created.

Unified Astronomy Thesaurus concepts: Comet nuclei (2160); Comet surfaces (2161); Meteor showers (1034); Meteor streams (1035); Spectroscopy (1558); Spectrophotometry (1556); Orbital evolution (1178)

1. Introduction

1.1. 2003 EH_1 and the Quadrantids

(196256) 2003 EH_1 (hereafter "EH_1") is the long searched for parent body of the Quadrantid meteor shower (Jenniskens 2004), an inactive near-Earth object (NEO) in a highly inclined Jupiter Family Comet (JFC)-like orbit. EH_1 is possibly related to C/1490 Y1, a previous suggested parent of the Quadrantid meteor shower (Hasegawa 1979). Another object, 96P/Machholz (hereafter 96P), has been been dynamically associated to the Quadrantids based on its orbital evolution (e.g., McIntosh 1990). Using the absolute magnitude of 16.1 listed on JPL's Small Body Database and a cometary albedo ($p_v \approx 0.03 - 0.06$), the diameter of EH_1 should be between 3.3 and 4.6 km (Kasuga & Jewitt 2015 estimate 4.0 ± 0.4 km), around the same size estimated for 96P (e.g., Eisner et al. 2019), making both objects larger than typical JFCs ($D \sim 1.3$ km, Meech et al. 2004; Bauer et al. 2017). Both objects have broadband colors more neutral (less red) than typical cometary nuclei (Kasuga & Jewitt 2015; Eisner et al. 2019), commonly interpreted as a possible signature of thermal effects on their surfaces. While 96P's orbit currently has $q \sim 0.1237$ au, the perihelion distance of EH_1 was similarly low ($q \sim 0.1$ au) within the past 2000 years (Jenniskens 2004; Wiegert & Brown 2005), making thermal changes to their surface seem plausible.

The Quadrantids appear to have a young (minimally dispersed) component ($\approx$200–600 years old) and an older (more dispersed) component ($\approx$1000 s of years old) (Jenniskens et al. 1997; Jenniskens 2004; Wiegert & Brown 2005; Babadzhanov et al. 2017). Jenniskens (2004) used these lines of evidence to argue that the younger component is the result of a breakup of a cometary precursor at some point in the past few hundred years. This is bolstered by 96P's modern-day disintegration and parenthood to the Marsden and Kracht sungrazing comet groups (see Marsden 2005; Battams & Knight 2017; Jones et al. 2017 for excellent reviews of the topic). Abedin et al. (2015) argued that the younger component can be well explained by traditional cometary activity that started on EH_1 in the 1790 s. The Quadrantid Complex of small bodies is thus something of a laboratory to study the ongoing processes of cometary activity, dormancy, thermal alteration, nuclear fragmentation and meteor shower creation.

1.2. Dormant Comets

The processes by which classical comets "turn off" and become dormant or inactive are of great interest, as a better understanding would shed light on the processes of resurfacing and physical evolution of devolatilized regolith, which have implications for the extent, depth, and evolutionary state of interior volatiles and may indicate any relationship to low-albedo NEOs. There are few direct spectroscopic observations of cometary nuclei in the literature for comparison with candidate dormant comets, as active comets may only have their surfaces seen directly when their activity is minimal (e.g., near aphelion), making these observations of low-albedo kilometer-sized objects even more challenging. Luu (1993) obtained spectra of several comet nuclei and dormant comet candidates at large heliocentric distances, and found a wide variety of spectral behaviors from weakly blue (95P/Chiron) to strongly red (10P/Tempel) among the proper comets, but a wider range of behaviors in the candidates from strongly blue ((3200) Phaethon) to "ultrared" ((5154) Pholus). While (3200) Phaethon is indeed the parent of the Geminid meteor shower (Whipple 1983), its status as a likely dormant comet has come

under serious scrutiny over the past decade (de León et al. 2010; Jewitt & Li 2010; see also Kareta et al. 2018). The ultrared surface of (5154) Pholus (see, e.g., Fink et al. 1992; Cruikshank et al. 1998) and other Kuiper Belt objects (KBOs) and Centaurs does not appear to occur on "normal" cometary nuclei (Jewitt 2002), either. Many likely comparison points for cometary nuclei may be at radically different stages of cometary evolution, from yet-to-activate Centaurs (e.g., Pholus) to long-since heated-and-devolatilized comets or carbonaceous asteroids (e.g., Phaethon, 107P/Wilson-Harrington, Fernández et al. 1997), making meaningful comparisons much more challenging. Nearly dormant or low-activity comets allow for a longer observational window when activity is minimized, and so far individual studies of the nuclei thereof (Licandro et al. 2003; Abell et al. 2005; Campins et al. 2006; Hicks & Bauer 2007) all show very red D-type-like spectra with little variation. Insights from Rosetta at comet 67P/Churyumov-Gerasimenko (Capaccioni et al. 2015; Oklay et al. 2016; Filacchione et al. 2019) suggest that reflectance spectra less red than the typical D-type slope on active comets could be caused by increasing ice content in the upper regolith, perhaps most relevant for Chiron of all the bodies mentioned so far, considering it is well beyond the where water would sublimate easily. That being said, Chiron's coma is bluer than the Sun (West 1991), so measurements of its nuclear properties that find it to be blue as well might be contaminated by a low surface brightness coma that was not noticed or fully subtracted, which seems like a plausible worry considering the inherent dimness of the object. With observations of all cometary surfaces, identifying whether or not the object is so active that determination of the nuclear properties is reasonable is critical.

A secondary issue is that the dynamical chaos of the inner solar system can make the modern orbital state of the object in question nondiagnostic in predicting its original reservoir (e.g., Main Belt versus Kuiper Belt). 2P/Encke might have spent time in Main Belt (Levison et al. 2006) despite a likely Kuiper Belt origin, while the recent work by Hsieh et al. (2020) shows that even active objects in JFCs orbits may potentially be active asteroid interlopers. The long-term dynamical and thermal evolution of these groups of bodies likely differ greatly, so diagnosing how their surfaces and interiors are responding to devolatilization is complicated without auxiliary information to constrain the possible options for investigation.

EH_1 is what one would "expect" a dormant comet to look like—it was likely quite active in the recent past (as recently as 100–200 years ago according to Abedin et al. 2015), it is associated with a meteor shower (the Quadrantids), and is genetically linked to other comets (96P, possibly C/1490 Y1). The goal of this paper is to leverage the ample auxiliary understanding we have of the Quadrantid complex to better understand how and when EH_1 became dormant, and thus better interpret observations of dormant and low-activty comets in general. For comparison with EH_1, we present new spectroscopic observations of three nearly dormant comets whose properties we describe here and in Table 1. 364P/Pan-STARRS is a nearly dormant near-Earth JFC whose surface properties have not been reported, but had a "maybe asteroidal" dynamical history according to Fernández & Sosa (2015). Notably, it was discovered without detectable activity only a few months prior to its 2013 perihelion (Buzzi et al. 2013). 249P/LINEAR is also a nearly dormant near-Earth JFC, which was reported by Fernández et al. (2017) to have a weakly blue (B-Type) surface based on spectra taken between 0.5 μm and 0.85 μm and a likely dynamical origin in the Main Belt, not the outer solar system. Those authors reported that 249P is active for ~20 days around perihelion and not elsewhere during its orbit. Lastly, P/2006 HR_{30} (Siding Spring) is a nearly dormant Halley-Type Comet (HTC) that was characterized spectrally in Hicks & Bauer (2007) and DeMeo & Binzel (2008) and found to have a typical cometary D-type-like reflectance spectrum between $\sim 0.3\mu m$ and $\sim 2.5\mu m$.

In Section 2, we detail our observations of EH_1 and these three low-activity comets. In Section 3, we preliminarily compare our measurements with each other and previous observations of these targets (where applicable). In Section 4, we present a series of short-term high-resolution orbital integrations and comment on the likely modern thermal state of these four objects. In Section 5, we discuss the origin of the spectral variation within our sample of cometary nuclei and make constraints on the recent history of the Quadrantid meteor shower and complex.

2. Observations and Data Reduction

We obtained these new observations of EH_1 and three nearly dormant comets were taken at a variety of telescopes between 2006 and 2019, the details of which are summarized in Table 2. Spectroscopic observations of (196256) 2003 EH_1 were obtained at Gemini South with the GMOS-S instrument (Hook et al. 2004; Gimeno et al. 2016) on 2019 December 2nd using the R150 (low resolution) grating and the blue-blocking G455 filter, resulting in a wavelength coverage of $\sim 0.50\mu m$ to $\sim 1.02\mu m$. BVRI photometric observations were obtained of EH_1 on 2014 February 20 at the 1.8 m Vatican Advanced Technology Telescope (VATT) on Mount Graham with the Vatt4k imager. A total of 61 images were taken in four filters (10 B, 10 V, 23 R, 8 I), all with an exposure time of 60 s. The Vatt4k is a back illuminated STA0500A CCD with 4096×4096 15×15 micron pixels, which was then binned 2×2 to yield a plate scale of 0.38 arcsec/pixel. 364P/Pan-STARRS was observed on 2018 September 19th with SpeX (Rayner et al. 2003) with the MORIS instrument (Gulbis et al. 2011) used for guiding on the NASA Infrared Telescope Facility (IRTF). Visible spectroscopic observations of P/2006 HR_{30} (Siding Spring) and 249P/LINEAR were obtained on 2006 November 25th with the FAST instrument (Fabricant et al. 1998) on the Fred Lawrence Whipple Observatory (FLWO) 1.5 m telescope. The 364P observations span $\sim 0.8\mu$m to $\sim 2.3\mu$m, the 249P observations from $\sim 0.45\mu$m to $\sim 0.74\mu$m, and HR_{30} from $\sim 0.43\mu$m to $\sim 1.0\mu$m. All spectroscopic observations were obtained at or near the parallactic angle to minimize any wavelength-dependent slit losses (e.g., Filippenko 1982). None of the objects were detectably active (extended or brighter than expected) during the observations, though that does not preclude low-level dust contamination as discussed in the Introduction.

The data were reduced using standard procedures. All frames were debiased and flat-fielded, and a dark current correction was applied when applicable. The spectroscopic observations of 364P, 249P, and P/2006 HR 30, as well as the photometric observations of EH_1, were processed into reflectance by direct comparison with a Sun-like star observed at very similar airmass. The SpeX observations of 364P also included a further correction to a true solar analog (SAO 93936, type G2V) after

Table 1
Observational Targets

Object Name	a (au)	e	i (deg.)	T_J	Notes
(196256) 2003 EH_1	3.123	0.619	70.84	2.065	Inactive JFC
364P/Pan-STARRS	2.877	0.723	12.16	2.814	Weak activity JFC
249P/LINEAR	2.776	0.816	8.43	2.709	Weak activity JFC
P/2006 HR_{30} (Siding Spring)	7.818	0.843	31.88	1.785	Weak activity HTC

Note. All orbital elements taken from JPL Horizons as queried 2020 May 15.

preliminary correction with a closer by telluric star (SAO 166215, type G5V). The GMOS-S observations were designed differently to better accommodate Gemini's queue-based scheduling system at the suggestion of the support astronomers, and were first flux-calibrated using an observation a flux-calibrated standard star (CD-32 9927) observed using an identical instrument configuration earlier in the semester, further calibrated using observations of other stars observed the same night (primarily to fix red-wavelength telluric absorptions), and then finally divided by the high-quality spectrum of the Sun in (Chance & Kurucz 2010). This procedure was viewed as an acceptable risk (as opposed to a direct observation of a Sun-like star) due the preexistence of photometry both presented in this paper and in (Kasuga & Jewitt 2015). The observations of 364P with SpeX were reduced using "spextool" (Cushing et al. 2004), the photometric observations of EH_1 and the spectroscopic observations of 249P and P/2006 HR_{30} were reduced in the IRAF environment, and the reductions of the GMOS-S EH_1 observations were done in Python using the AstroPy (Astropy Collaboration et al. 2013, 2018) package.

The spectra are all shown to be distinct and the photometry of EH_1 is seen to agree well with the spectrum retrieved.

3. Observational Results

3.1. The Surface of (196256) 2003 EH_1

The left-hand panel of Figure 1 shows the first-ever reflectance spectrum of Quadrantid parent (196256) 2003 EH_1 along with photometry from a previous apparition. The spectrum presented is a median combination of the four individual spectra combined together in 100 $\AA$ bins. The spectrum is seen to be red-sloped and linear below approximately ~8000 Å and blue sloped beyond out to 1.02μm. The measured colors from our 2014 imaging, $B-V=0.65\pm0.04$, $V-R=0.33\pm0.03$, and $R-I=0.45\pm0.03$, are very similar to the colors of the Sun (Willmer 2018) and the colors of Kasuga & Jewitt (2015). The retrieved reflectance spectrum and photometry agree at the 1σ level or better, though the photometry is generally noisier than the spectrum. The right-hand panel of Figure 1 compares EH_1's spectrum with the D, S, C, and B asteroid taxonomic classes of DeMeo et al. (2009). At wavelengths shorter than $\sim 8000\,\AA$ (approximately the "I" filter), the spectrum is shown to be featureless and intermediate in "redness" between the C and D types as inferred from the photometry of Kasuga & Jewitt (2015). The bluer slope beyond that $\sim 8000\,\AA$ is dissimilar from the silicate absorption feature common on rocky asteroids like S-types, as the band center near 9000 Å would be well captured in the data if it were there.

EH_1's spatial full-width half-max (FWHM) is 0.″6 (averaged over wavelength), identical to other stars in the slit, and no signatures of gas emission (e.g., C_2's bandhead at $\sim 5167\,\AA$) are seen above the noise level. In general, we have strong confidence that the object was not detectably active and our retrieved reflectance spectrum reflects the actual properties of this dormant comet nucleus. To properly compare EH_1 and our other targets with previous observations of comet nuclei, we adopt the S' framework ("normalized reflectivity gradient," Luu & Jewitt 1990) whereby we report slopes as:

$$S'_\lambda(\lambda_1, \lambda_2) = (dS/d\lambda)/S_\lambda$$

Where λ_1, λ_2 are the starting and ending wavelengths, $(dS/d\lambda)$ is the best-fit linear slope over the region, and S_λ is the reflectivity measured at the central wavelength of the range. This normalized slope is commonly reported in $\%/0.1\mu m$. We attempt to capture the curvature of these cometary spectra by fitting the slope over several ranges: 0.5μm–0.7μm, 0.7μm–0.85μm, 0.85μm–1.0μm, 1.0μm–1.5μm, and 1.5μm–2.0μm. We report the fit S' values in Table 3 for all targets, as well as the same procedure applied to the Bus-Demeo (DeMeo et al. 2009) "C" and "D" taxonomic classes for reference.

While the interpretation of EH_1's spectrum is the Discussion section, two points may be made here. First, as we did not a priori expect EH_1's spectrum to have any deviations from linear and red-sloped based on our and other's photometry, we thoroughly inspected all aspects of our data reduction pipeline to look for any part that could have introduced such a feature. We were not able to find any plausible cause, which when combined with the fact that the Python pipeline can successfully reproduce the results of the Gemini-specific IRAF packages greatly increases our confidence in it. (Furthermore, there are other comet-adjacent objects that actually look similar, see the Discussion.) Secondarily, the decrease in flux below 5000 $\AA$ is possibly calibration related, as the choice of grating (R150) and spectroscopic blocking filter (G455) makes the flux plummet between 4600 Å and 4900 Å. As a result, we cut all data below 5000 $\AA$ as we could not verify that its relative calibration was accurate. The remaining data agrees well with our photometric measurements.

3.2. Other Cometary Surfaces

The spectral slopes fit over the same ranges of wavelength for our other comets, 364P/Pan-STARRS, 249P/LINEAR, and P/2006 HR_{30} (Siding Spring) are also listed in Table 3. The spectra of all four cometary nuclei, including EH_1 are plotted in Figure 2. Our retrieved spectrum for HR_{30} is without question much redder than the other objects in our sample, and while Hicks & Bauer (2007) do not quote a value for S', our spectrum seems consistent with their spectrum and photometry. (They report it as being slightly redder than a typical D-type, which is consistent with our data.) The spectrum retrieved for 364P, for

Table 2
Observation Log

Object Name	UTC Date, Time[a] (yyyy mm dd)	Telescope, Inst.	Exp. Time (s)	R_H, Δ (au)	P.A. (deg.)
(196256) 2003 EH_1	2019 Dec 02, 6:12	Gemini S., GMOS-S	4×900	1.491, 1.496	39.9
"	2014 Feb 20, ~3:00	VATT, VATT4k	51×60	1.22, 1.15	52.3
364P/Pan-STARRS	2018 Sep 19, 11:46	IRTF, SpeX, MORIS	18×200	1.505, 0.540	17.8
249P/LINEAR	2006 No 25, 7:04	FLWO 1.5 m, FAST	2×900	1.609, 0.626	5.1
P/2006 HR_{30} (Siding Spring)	2006 Nov 25, 2:16	FLWO 1.5 m, FAST	2×900	1.339, 0.927	47.4

Note.
[a] At exposure start.

which no reflectivity has been reported before, is weakly red throughout the entire wavelength range considered, and is consistent with either linear from 7500 Å onward or perhaps being slightly redder at longer wavelengths (>20000 Å $= 2.0\mu m$). The heliocentric distance at the time of observation, $R_H = 1.505$au makes the longer wavelength upturn (again, at the limit of the data) unlikely to be from thermal emission from 364P's nucleus (Rivkin et al. 2005; Reddy et al. 2009, 2012; Kareta et al. 2018), as the subsolar temperature would be ~320 Kelvin (assuming a Bond Albedo of $A \sim 0.03$), which is likely too low to affect the spectrum. The spectrum of 249P is weakly red and linear throughout the entire observed range ($\sim 0.45\mu$m– $\sim 0.74\mu$m). Observations when the object was more active by Fernández et al. (2017) showed a linear and gently blue-sloped ($S' \sim -2.0$) reflectance spectrum.

To facilitate better comparison with the literature, we also performed a direct χ^2-test directly comparing the Bus-Demeo (DeMeo et al. 2009) taxonomic classes with each of our spectra. The results agree with the preliminary assessment given through the slope analyses in Table 3: 249P and 364P are both equally well fit as C or Cgh class objects, the best fit to HR_{30} is a D-type but the template spectrum is noticeably not red enough at visible wavelengths, and EH_1 is best fit as a C-type, but none of the spectral classes make a great match.

4. Recent Orbital Evolution

4.1. Orbital Integration

As discussed in the Introduction, one key piece of information that is critical to interpreting the modern state of a cometary nucleus is understanding how its orbit has changed recently. Was the comet in question a sungrazer at some point in the recent past, or was it only recently injected from a Centaur-like orbit? Has it had a particularly close encounter with a planet that might have resurfaced it (Binzel et al. 2010)? A short-term orbital integration can answer these questions (within the uncertainties of the orbit solution) and is an invaluable tool to placing these small body observations within the proper context.

While EH_1's (Jenniskens 2004; Wiegert & Brown 2005; Babadzhanov et al. 2017) and 249P's (Fernández et al. 2017) recent orbital evolution have been studied, 364P and HR_{30} lack the same characterization. For completeness, we numerically integrate all four of our observed bodies identically using the following methodology. Using the REBOUND (Rein & Liu 2012) package in Python with the IAS15 (Rein & Spiegel 2015), the planets Mercury through Neptune, and a nominal timestep of 0.0001 years (approximately 52.6 minutes), we integrated the nominal orbits of of four targets as well as 100 clones each drawn from the orbital uncertainty covariance matrices on the JPL Small Body Database back in time 2000 years. As all objects have either weak or no activity, no nongravitational effects were included, and the 2000 yr time frame was chosen to reflect the fact that their activity patterns were certainly different in the past. (For EH_1 in particular, this is an especially large unknown.) The results of these orbital integrations are shown in Figure 3. We used the most recent orbital solutions and associated error matrices from JPL Horizons as available in the Summer of 2020. In order, they were number 33 for EH_1, number 48 for 364P, number 32 for 249P, and 87 for HR_{30}. If a reader wanted to duplicate or expand upon this work, they should verify that the orbital solution they use is the same as what we have used here, or ideally a newer and more precise solution than we had available. For context and comparison with EH_1, we also integrated the recent motion of 96P/Machholz using the same methodology and the JPL orbit solution K173/5.

4.2. Results of Integrations

While all four objects are currently dormant or nearly dormant comets in near-Earth space, they have, as expected, undergone very different orbital evolutions over the past two thousand years. The "bumpiness" in Figure 3 is due to moderately distant ($d \geqslant 1.0 R_{\rm Hill}$) or further encounters with Jupiter, and no significant encounters with the Earth were noted. (See the Appendix for a Figure showing these distances as a function of time.) EH_1's behavior here is largely identical to previous studies (Jenniskens 2004; Wiegert & Brown 2005; Babadzhanov et al. 2017) where it is retreating outward from a sungrazing orbit. Of the 100 clones considered, the minimum perihelion distance ranged from $q = 0.082$ au to $q = 0.109$ au with a median (as in, the median of all 100 minimum q values) of $q = 0.0981$ au. EH_1's orbit and 96P's orbital evolution are strikingly similar as previously studied, with both objects oscillating between moderate and extreme eccentricities through the Kozai mechanism. (The reader is referred to previous studies for a more in-depth discussion of their orbital configuration and relationship, e.g., Sekanina & Chodas 2005.) 364P and 249P are both currently decreasing their perihelion distances. 364P's current value($q = 0.798$ au) is only marginally larger than its median minimum of $q = 0.775$ au. 364P's orbital clones begin to spread more noticeably than the other object studied, with one clone reaching a minimum q of 0.647 au. 249P's current $q = 0.509$ au is only barely larger than its historical minimum of $q = 0.503$ au in 1997. HR_{30}'s evolution is perhaps the least interesting, as its perihelion distance has been slowly increasing over the entire time frame

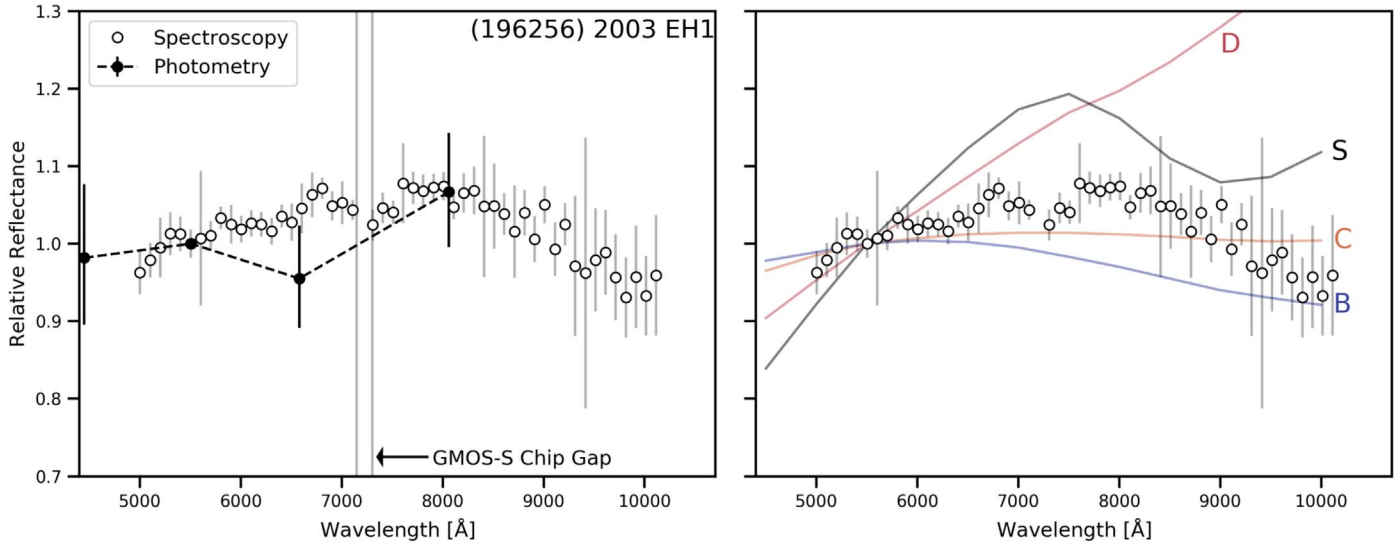

Figure 1. Left: the reflectance spectrum of (196256) 2003 EH_1 is shown (black unfilled circles, errors shown as shaded area) and new BVRI colors from a different apparition (2014) converted into reflectance using the Solar colors of Willmer (2018) (black filled circles, errors shown as vertical error bars). The spectrum and photometry were normalized at *V*-band (5510 Å). The space between CCDs presents a ∼ 150 Å gap in wavelength coverage. The photometry and spectrum agree at the 1σ level or better. The reflectance spectrum of EH_1 is shown to be mildly red below ∼8000 Å and blue at longer wavelengths. Right: the same spectrum of EH_1 plotted against the D, S, C, and B asteroid taxonomic classes of DeMeo et al. (2009). The slope of the object is intermediate in "redness" between the C and D types below ∼8000 Å as previously reported by Kasuga & Jewitt (2015), and the downturn at longer wavelengths is discussed at length in the text.

considered from its minimum $q = 1.082$ au to its modern $q = 1.226$ au. (Even this modest change in q results in a 22% decrease in input solar energy.) In general, EH_1 is retreating from a sungrazing orbit, 364P and 249P are slowly warming as their perihelion distances continue to decrease, and HR_{30} is somewhat colder than it was 2000 years ago.

To understand their modern thermal states more quantitatively, we now compute the change in surface temperatures for each of the four objects under the following assumptions. We calculate the subsurface temperature at perihelion, $T_{SS,q}$, as a proxy for the maximum temperature sustained on the object and thus the most extreme thermal conditions where thermal metamorphosis of surface materials and volatile sublimation would be most preferred. Following the formulation from the near-Earth asteroid thermal model (NEATM; Harris 1998):

$$T_{SS,q} = \left[\frac{(1-A)S_{\odot}}{(\eta\epsilon\sigma_{SB}) \times q_{au}^2}\right]^{1/4} \quad (1)$$

where A is the bond albedo (taken to be 0.02), $S_{\odot}$ is the Solar constant (1361 Wm^{-2}), η the "infrared beaming parameter" (technically unknown, taken to be 1.1), ϵ is the infrared emissivity of the object (taken to be 0.9), σ_{SB} is the Stefan-Boltzmann constant, and q_{au} is the perihelion distance of the object in au. Plugging in all of these numbers, the equation simplifies to $T_{SS,q} = 373\text{K} \times q^{-1/2}$. EH_1's modern perihelion is at ∼1.19 au, making $T_{SS,q} = 341$K, while at its historic low of ∼0.098 au some 1500 years ago, it was radically hotter at $T_{SS,q} = 1192$K. The other objects in this study do not come close at all to comparing. 249P and 364P are both at or near their hottest temperatures within the last few thousand years, with values of $T_{SS,q} = 524$K (249P) and $T_{SS,q} = 422$K (364P). In both of these cases, this is likely an *overestimate* of their actual perihelion maximum temperatures, as they clearly still undergo some mass loss that would cool the surface under the safe assumption it is driven by ice sublimation. HR_{30}'s historically hottest temperature within the studied time frame is $T_{SS,q} = 359$K, only barely hotter than EH_1's modern values. While these values are imprecise to be certain (comets do not have uniform albedos for one, and the worry that intense solar heating might have changed the thermal properties of EH_1's surface seems like a reasonable concern, among other caveats), EH_1's thermal history is really not similar to these other objects, despite their similar evolutionary states from the perspective of how recently they were active and at what level. 249P and 364P today have similar temperatures to what EH_1 would have had in the past few hundred years, but it is worth clarifying that EH_1 got there by cooling down while 249P and 364P are still warming up, and thus it may not be an apples-to-apples comparison.

5. Discussion

5.1. The Surface of 2003 EH_1

The reflectance spectrum of EH_1, red below $\sim 8000\,\AA$ and blue at longer wavelengths, is surprising, but not unprecedented. Setting aside that BVRI photometry alone leaves observers blind to such spectral behavior, the study of Tubiana et al. (2015) showed clearly that there were a variety of shapes that reflectance spectra of possibly dormant-comet-NEOs can present in the $0.7 - 1.0\mu m$ range. In particular, the qualitative similarity between EH_1 and their spectra of 2P/Encke (and associated inactive NEOs 1998 QS_{52}, 1999 RK_{45}, 2003 QC_{10}, and 2003 UL_3) is interesting. In Figure 4, we show a comparison of our data on EH_1 with that of 2P/Encke, 1998 QS_{52} and 1999 RK_{45} from Tubiana et al. (2015) as produced from the raw data of their observations available on the ESO archive. A red-sloped visible spectrum is seen to become neutral or even partially blue around the same wavelengths considered. If EH_1 and 2P/Encke look similar, it seems likely that many low-perihelion cometary objects might have nuclear spectra that look like these objects. This is bolstered by measurements of 96P's nuclear colors Eisner et al. (2019), which suggest that it too has a less-red-than-a-D-type surface

Table 3
Spectral Slopes

Object Name	0.5–0.7[a]	0.7–0.85[a]	0.85–1.0[a]	1.0–1.5[a]	1.5–2.0[a]
(196256) 2003 EH_1	3.9 ± 0.5	2.2 ± 0.8	$0^{\cdot} \pm 2.0$		
364P/Pan-STARRS		1.0 ± 1.0	3.8 ± 0.5	1.4 ± 0.3	1.2 ±minus7 0.9
249P/LINEAR	1.1 ± 0.3				
P/2006 HR_{30} (Siding Spring)	13.9 ± 0.2	5.9 ± 0.4	5.0 ± 1.0	3.5 ± 0.1	2.8 ± 0.2
Bus-Demeo C-type[b]	1.5 ± 0.3	-0.3 ± 0.1	-0.4 ± 0.2	0.8 ± 0.1	1.8 ± 0.1
Bus-Demeo D-type[b]	8.4 ± 0.2	5.9 ± 0.3	7.2 ± 0.2	4.6 ± 0.1	2.5 ± 0.1

Notes.
[a] Wavelength range in μm, slope in $\%/0.1\mu m$
[b] These are the standard taxonomic C and D classes from DeMeo et al. (2009), and thus represent an average of the reflectivities of several input objects.

similar to EH_1 and Encke. While both the pyroxene band at $\sim 0.9\mu$m and the hydration feature at $\sim 0.7\mu$m would be well resolved by our data set, both olivine and magnetite have absorptions centered near $\sim 1.0\mu$m that could plausibly be the origin of the spectral downturn (see, e.g., the study of Yang & Jewitt (2010) on the origin of B-type slopes) that may not be resolved by the current data set. Many carbonaceous chondrites, especially the heat-processed CI and CM chondrites, show absorption features in this region with band centers that are near $\sim 1.0\mu$m (see discussion of curve matching of meteorites to cometary nuclei in Abell et al. 2005; Filacchione et al. 2019), often attributed to magnetite. Recently magnetite was found in samples of 81P/Wild 2 by Hicks et al. (2017). The taxonomic classification of EH_1 with our spectrum (a C-type) would generally support this line of thinking (even the C-type spectrum template has a wide weak dip near $\sim 1.0\mu$m), but we note again that EH_1 is still too red at visible wavelengths and the dip near $\sim 1.0\mu$m too strong to really fit a C-type spectrum well. The spectra of Encke-related NEOs in Tubiana et al. (2015) are generally redder than EH_1 with slope changes/absorption features much weaker that shown here, and thus could fit to S/Sq/Q types more easily than the more neutrally colored Quadrantid parent. We have reason to believe the surfaces our similar, without question, but they do differ in the details. That said, without longer wavelength characterization and confirmation of this feature, it is challenging to ascertain its origin. de León et al. (2012) found that many B-type asteroids have slope changes in this region that are not clearly observed as "bands" on the objects in question. In summary, the decrease of EH_1's reflectivity at longer wavelengths could plausibly be related to olivine or magnetite but without longer-wavelength data it is not possible to rule out other options.

In addition to both confirmation of the reflectance decrease found here on EH_1, better and longer-wavelength spectroscopic characterization of the surfaces of other near-Sun bodies could be quite useful in characterizing the changes undergone as they heat and change. Nuclear spectra of 96P, while undoubtedly challenging observationally, would be incredibly useful. Another future path to explore would be to obtain near-infrared observations of EH_1 and the Encke-associated bodies. It appears that such data was taken for Encke (Abell et al. 2009) but remains thus far unpublished. We had planned near-infrared observations of EH_1 also to be taken at Gemini South, but unplanned instrumental maintenance removed FLAMINGOS-2 (Eikenberry et al. 2006) from active use throughout most of our observational window. Regardless, the fact that the two best-studied low-perihelion comets, 96P/Machholz and 2P/Encke as well as many of their associated NEOs including 2003 EH_1 have more neutral reflectance spectra than typical cometary nuclei is certainly compelling, and could prove quite useful in identifying other dormant comet NEOs.

5.2. Spectral Properties of Dormant and Low-activity Comets

The variety of spectra seen in our barely active comet sample is similar to what other authors (Luu 1993, see, e.g.) have measured. The spectra are red-sloped to varying degrees without obvious features. HR_{30} shows slight curvature near 8000 $\AA$, also seen on other comets like 67P (Capaccioni et al. 2015; Filacchione et al. 2019) and C/2001 OG108 (LONEOS) (Abell et al. 2005) as well as D-type asteroids. 364P's more neutral but still largely linear spectrum is within the range of slopes expected for cometary nuclei from Luu (1993), but there are very few cometary nuclei which have been studied spectroscopically at similar near-infrared wavelengths, so direct comparisons are few. C/2001 OG108 (LONEOS) (Abell et al. 2005) and 124P/Mrkos (Licandro et al. 2003) both have similar D-type-like slopes in the near-infrared, but it is hard to directly compare those as well without complementary visible observations. Abell et al. (2005) does present visible colors of OG108, which shows it to be on the less-red end of the observed population of comet nuclei, while the colors of Hicks & Bauer (2007) show HR_{30} to be on the redder end. In other words, OG108 and 364P are both primarily linear over the near-infrared range and both appear to be less red than HR_{30}. 249P's largely featureless and red-sloped spectrum would not be particularly notable if it was not for the previous observation of it by Fernández et al. (2017) which showed it to be featureless and slightly blue. While such a small difference in slope ($\Delta S' \sim 3 - 5$) could in principle be due to something like improper or inconsistent calibration of either or both data sets, another option is that their retrieved spectrum is simply more contaminated by dust than assumed. 249P is often seen with a distinct tail but little noticeable coma, so contamination might be more challenging to detect, even if it is minimal. The similar reflectance spectra of 249P and 364P, when combined with their very similar recent orbital evolutions and possibly similar origins in the Main Belt (Fernández & Sosa 2015; Fernández et al. 2017), suggest strongly that these objects have similar surface properties developed through similar processes.

5.3. The Recent History of 2003 EH_1 and the Quadrantid Meteor Shower

EH_1. EH_1 is thought to have produced the Quadrantids within the past 200–300 years (Wiegert & Brown 2005) and is not detectably active today. The dynamics of this situation make the story more confusing still: if EH_1's perihelion

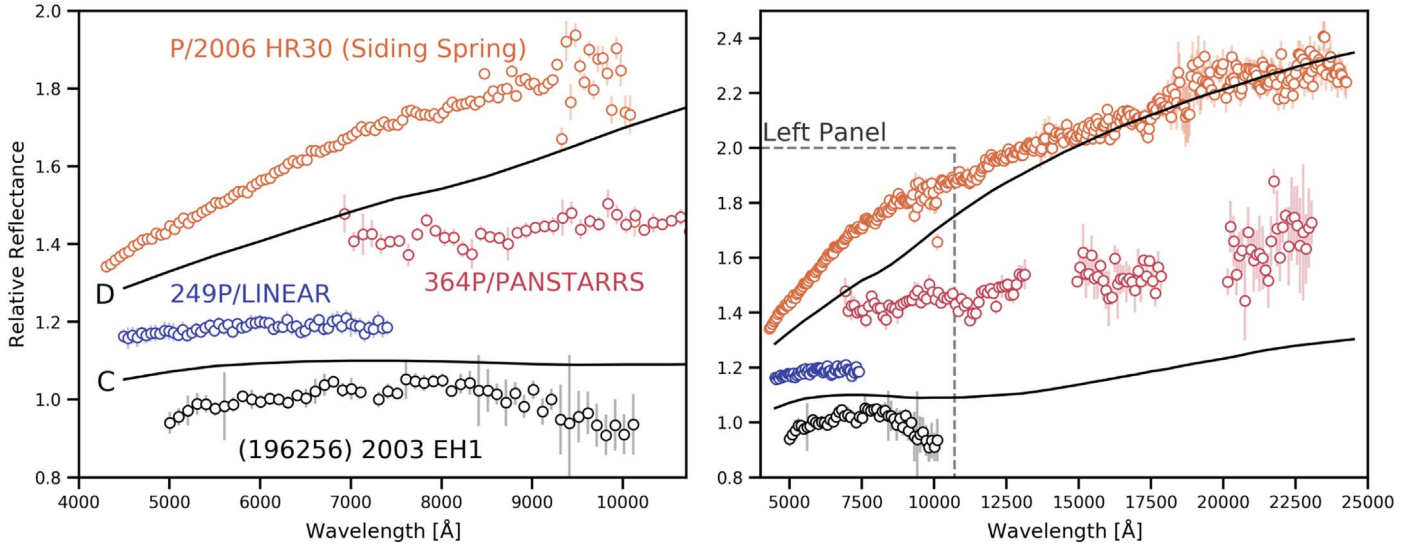

Figure 2. Reflectance spectra of P/2006 HR_{30} (Siding Spring), 364P/Pan-STARRS, 249P/LINEAR and (196256) 2003 EH_1 are shown normalized at 7300 Å and offset from each other vertically for clarity. The left-hand panel is a zoom in to the "visible" range of wavelengths, while the right-hand panel shows both visible and near-infrared wavelengths. In the right-hand panel, our spectrum of HR_{30} is combined with that of DeMeo & Binzel (2008) for better comparison with 364P. The Bus-Demeo C- and D-type spectra are plotted similarly for context. All four cometary nuclei are shown to be red at visible wavelengths, with HR_{30} becoming slightly more neutral near 8000 Å, EH_1 becoming blue, and no slope change being seen in the region for 364P. 249P is essentially linear throughout the entire wavelength range considered.

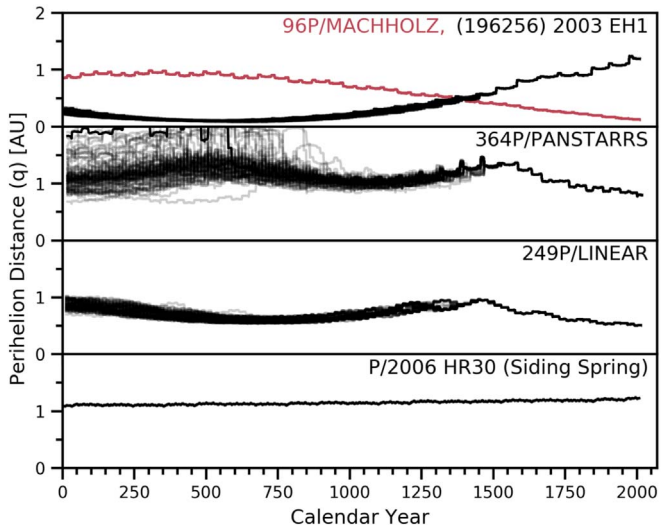

Figure 3. Evolution of perihelion distances (q) for (196256) 2003 EH_1, 364P/Pan-STARRS, 249P/LINEAR, and P/2006 HR_{30} (Siding Spring) (top to bottom) over the past 2000 years. The nominal orbit and the orbits of 100 clones each are shown, with the clones plotted in the same black color but partially transparent. The comet 96P/Machholz is included for comparison with EH_1 considering the similarities of its orbit with that of EH_1. The details of the integrations are described in the text.

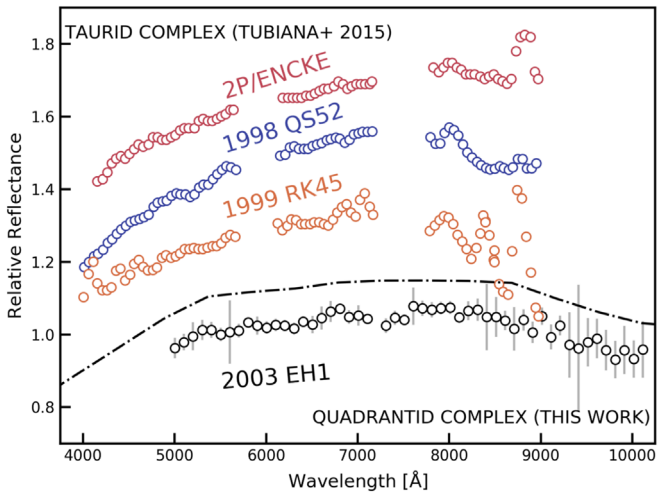

Figure 4. Reflectance spectra of 2003 EH_1 (black, from this work) and of three members of the Taurid Complex from Tubiana et al. (2015). While EH_1 is more neutrally colored than these handful of Taurids-related objects, the qualitative similarity of these multiple comet/meteor shower-related/low-perihelion objects showing similar objects is clear. While all objects considered are red until $0.75 - 0.8\mu$m, all are neutral or blue at longer wavelengths, errors considered.

distance was ~0.1 au 1500 years ago, why are the Quadrantids from a thousand years after when it was significantly colder? If it was active just 200–300 years ago, was its modern surface not "reset" by that activity? Why did EH_1's precursor object disintegrate and leave EH_1 inactive while 96P, at a similar size and presumably released even earlier, continues to be strongly active?

One line of evidence comes from the distribution of meteor masses (and thus sizes) in the Quadrantids stream which was noted by Blaauw et al. (2011) to have a lower mass index, along with the Geminids, than the other major showers studied. While having a lower mass index is both an indicator of formation age and formation process, the fact that the two best-studied meteor showers with (currently) inactive parent bodies have similarly distinct mass distributions compared with other showers is curious. In their numerical model of the formation of the Geminids, Ryabova (2016) suggests that certain aspects of the duration and timing of the meteor shower can only be explained if the orbit of the parent body—(3200) Phaethon—changed significantly during stream formation, perhaps as a result of intense and sudden outgassing. This hypothesis was first raised by Lebedinets (1985). If the similarity in properties of the Geminids and Quadrantids reflects something about their formation conditions (as opposed to coincidental subsequent

effects), then perhaps both streams formed from the violent breakup of a volatile-rich precursor. The breakup would cause the volatile-rich insides of the objects to start outgassing rapidly, leaving behind volatile-depleted bodies on slightly different orbits. This scenario seems highly likely for EH_1, considering that it was likely active just 200 years ago (Abedin et al. 2015) and that Wiegert & Brown (2005) found that EH_1's orbital elements differ slightly from those of C/1490 Y1, suggesting at least a moderate orbital change during stream formation seems likely if the two objects are indeed related. Direct comparison of models of the formation of the Phaethon-Geminid Complex with the Machholz/Quadrantid Complex seems like a promising avenue for future research into understanding the physical properties of their constituent bodies (see the comparison of the two complexes in Kasuga & Jewitt 2019), especially prior to the arrival of DESTINY+ Arai et al. (2018) at Phaethon in the late 2020 s.

EH_1's orbit over the past two hundred years has it with a similar perihelion distance to other objects in this study which it does not appear spectrally similar to (especially in terms of spectral curvature), suggesting that the ongoing processes on these other nearly dormant comets cannot likely produce an EH_1 spectrum at its current distance in the time elapsed assuming that they are made from similar materials. (For example, if 249P or 364P is indeed from the Main Belt, then it has likely experienced a totally different set of processes before even entering near-Earth space, and thus would not be expected to have very similar composition at the near-surface.) If similar objects in "colder" orbits cannot reproduce EH_1's spectrum, one explanation is that EH_1's surface, somehow, still records some evidence of the intense solar heating it received a thousand years ago. EH_1's rare-by-comet-standards reflectance spectrum is thus a combination of the processes that heated it intensely and then the processes that lead to its precursor object breaking up. If the Quadrantids were formed through normal cometary activity on EH_1 as recently argued by Abedin et al. (2015), then either the activity barely modified the remnant surface processes or only affected some fraction of the surface. This seems somewhat challenging to reconcile with the large mass of the stream, which is comparable to the mass of the object itself Kasuga & Jewitt (2015). If this hypothesis could be tested or backed up through other means (e.g., more complicated models of stream formation incorporating break-ups or only localized activity, laboratory work to see if EH_1-like spectra can be produced through the heating of cometary analogs, etc.), then our understanding of the actual process that created the Quadrantids could be greatly improved. EH_1

6. Summary

The parent of the Quadrantid meteor shower, (196256) 2003 EH_1, is a currently inactive near-Earth object that was likely active within the past ~200 years (Abedin et al. 2015). It is possibly a fragment of or genetically related to C/1490 Y1, dynamically associated with the active sungrazing comet 96P/Machholz, and previously was a sungrazer itself. EH_1 is thus not just a great opportunity to study a comet that has only recently "shut off" to better understand cometary dormancy (and the NEO population), but also the competing effects of intense thermal heating, fragmentation, and meteor shower production. However, compared with the other well-known inactive meteor shower parent body (3200) Phaethon, EH_1's surface properties have only been studied through broadband color measurements (Kasuga & Jewitt 2015). In this work, we present the first reflectance spectrum of EH_1 taken at Gemini South in December 2019 as well as new reflectance spectra of three nearly dormant comets: 249P/LINEAR, 364P/Pan-STARRS, and P/2006 HR_{30} (Siding Spring) for comparison. EH_1's surface is featureless, red, and intermediate in slope between the C and D taxonomic types until $\sim 0.8\mu$m as previously reported, but is blue (decreasing reflectivity as a function of wavelength) beyond up to at least $\sim 1.02\mu$m. The nearly dormant Halley-type comet HR_{30} has a classic cometary nucleus spectrum similar to a D-type asteroid, while the nearly dormant Jupiter family comets 249P and 364P both have more weakly red spectra similar to a C-type asteroid. This is more spectral diversity than expected for these objects considering their similarly low-activity levels. We also performed short-duration high-resolution orbital integrations for each object to infer how their thermal state has changed in the past 2000 years. While EH_1 is retreating from a sungrazing orbit as expected, HR_{30} has remained relatively stable with a perihelion near ~1 au. 249P and 364P have very similar orbital histories in terms of perihelion distance evolution, which combined with their similar surfaces suggests that similar processes have acted on both. A previous study of 249P suggested that it had a dynamical origin the main belt (Fernández et al. 2017), so a study similar for 364P could be critical in seeing how far their similarity goes. If EH_1's reflectance downturn is an absorption feature instead of a slope-break, then magnetite or olivine (but not pyroxene or the $\sim 0.7\mu$m hydration feature) could be responsible. Future studies of EH_1 at near-infrared wavelengths could both confirm the feature and shed light on its origin. Through comparison with the other objects in this study, we interpret the feature as a likely signature of relic thermal alteration on its surface, which is puzzling considering that the object likely fragmented and remained active between when it was in such a hot orbit and the present day. Understanding the origin of EH_1's surface properties should be useful in establishing a better understanding of how the Quadrantids were actually produced.

We thank two anonymous reviewers for helpful comments that improved the quality of the manuscript significantly. We thank Benjamin N.L. Sharkey and John W. Noonan for helpful discussions regarding the reduction of the various data sets. We would also like to thank Dr. Juan Sanchez for assistance in obtaining the IRTF observations of 364P/Pan-STARRS.

This research work was supported in part by NASA Near-Earth Object Observations grant NNX17AJ19G (PI: Reddy). We thank the IRTF TAC for awarding time to this project, and to the IRTF TOs and MKSS staff for their support. The authors wish to recognize and acknowledge the very significant cultural role and reverence that the summit of Maunakea has always had within the indigenous Hawaiian community. We are most fortunate to have the opportunity to conduct observations from this mountain. Part of the data utilized in this publication were obtained and made available by the MITHNEOS MIT-Hawaii Near-Earth Object Spectroscopic Survey. The IRTF is operated by the University of Hawaii under Cooperative Agreement no. NCC 5-538 with the National Aeronautics and Space Administration, Office of Space Science, Planetary Astronomy Program. The MIT component of this work is supported by NASA grant 09-NEOO009-0001, and by the National Science

Foundation under grants Nos. 0506716 and 0907766. Based on observations obtained at the international Gemini Observatory, a program of NSF's NOIRLab, which is managed by the Association of Universities for Research in Astronomy (AURA) under a cooperative agreement with the National Science Foundation. on behalf of the Gemini Observatory partnership: the National Science Foundation (United States), National Research Council (Canada), Agencia Nacional de Investigación y Desarrollo (Chile), Ministerio de Ciencia, Tecnología e Innovación (Argentina), Ministério da Ciência, Tecnologia, Inovações e Comunicações (Brazil), and Korea Astronomy and Space Science Institute (Republic of Korea).

All data products are available upon reasonable request to the corresponding author, and the unreduced observations of (196256) 2003 EH_1 from Gemini South are available at the Gemini Science Archive with Program ID GS-2019B-Q-308.

Facilities: Gemini (GMOS-S), IRTF (SpeX, MORIS), FLWO 1.5 m (FAST).

Software: NumPy (Harris et al. 2020), SciPy (Virtanen et al. 2020), AstroPy (Astropy Collaboration et al. 2013, 2018).

Appendix

Figure 5 shows the recent distances between Jupiter and the four observational targets in this study to expand on a brief point made in Section 4.

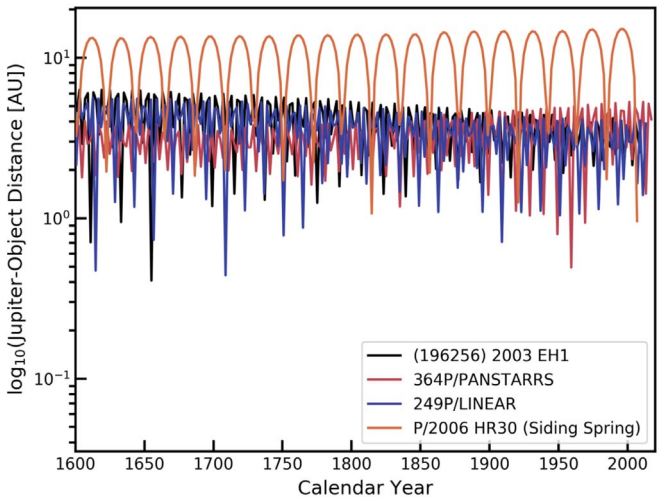

Figure 5. Evolution of each of our objects distances from Jupiter as output at each written timestep of the simulation with each of the four objects plotted in the same colors as they are in Figure 2. (EH_1 is black, 249P is blue, 364P is red, and HR_{30} is orange.) The "bumps" in the orbital evolution shown in Figure 3 for the non-HR_{30} objects all correspond with their orbital alignments with Jupiter shown in this plot. Of the four objects, 249P and 364P are much more likely to encounter Jupiter at a distance comparable with its Hill Radius due to their low inclinations. EH_1's high inclination and HR_{30}'s orbital classification as a Halley-type object make strong encounters less likely. A similar plot made with the Earth shows even fewer more distant encounters, though it is worth noting to future observers that 249P will approach the Earth quite closely at ~0.056 au in 2029.

ORCID iDs

Theodore Kareta https://orcid.org/0000-0003-1008-7499
Vishnu Reddy https://orcid.org/0000-0002-7743-3491
Walter M. Harris https://orcid.org/0000-0002-8378-4503

References

Abedin, A., Spurný, P., Wiegert, P., et al. 2015, Icar, 261, 100
Abell, P., Fernandez, Y. R., Lisse, C. M., Bus, S. J., & Schleicher, D. G. 2009, AAS Meeting, 41, 20.02
Abell, P. A., Fernández, Y. R., Pravec, P., et al. 2005, Icar, 179, 174
Arai, T., Kobayashi, M., Ishibashi, K., et al. 2018, LPSC, 49, 2570
Astropy Collaboration, Price-Whelan, A. M., Sipőcz, B. M., et al. 2018, AJ, 156, 123
Astropy Collaboration, Robitaille, T. P., Tollerud, E. J., et al. 2013, A&A, 558, A33
Babadzhanov, P. B., Kokhirova, G. I., Williams, I. P., & Obrubov, Y. V. 2017, A&A, 598, A94
Battams, K., & Knight, M. M. 2017, RSPTA, 375, 20160257
Bauer, J. M., Grav, T., Fernández, Y. R., et al. 2017, AJ, 154, 53
Binzel, R. P., Morbidelli, A., Merouane, S., et al. 2010, Natur, 463, 331
Blaauw, R. C., Campbell-Brown, M. D., & Weryk, R. J. 2011, MNRAS, 414, 3322
Buzzi, L., Bressi, T. H., Bosch, J. M., et al. 2013, MPEC, 2013, 15
Campins, H., Ziffer, J., Licandro, J., et al. 2006, AJ, 132, 1346
Capaccioni, F., Coradini, A., Filacchione, G., et al. 2015, Sci, 347
Chance, K., & Kurucz, R. L. 2010, JQSRT, 111, 1289
Cruikshank, D. P., Roush, T. L., Bartholomew, M. J., et al. 1998, Icar, 135, 389
Cushing, M. C., Vacca, W. D., & Rayner, J. T. 2004, PASP, 116, 362
de León, J., Campins, H., Tsiganis, K., Morbidelli, A., & Licandro, J. 2010, A&A, 513, A26
de León, J., Pinilla-Alonso, N., Campins, H., Licandro, J., & Marzo, G. A. 2012, Icar, 218, 196
DeMeo, F., & Binzel, R. P. 2008, Icar, 194, 436
DeMeo, F. E., Binzel, R. P., Slivan, S. M., & Bus, S. J. 2009, Icar, 202, 160
Eikenberry, S., Elston, R., Raines, S. N., et al. 2006, Proc. SPIE, 6269, 626917
Eisner, N. L., Knight, M. M., Snodgrass, C., et al. 2019, AJ, 157, 186
Fabricant, D., Cheimets, P., Caldwell, N., & Geary, J. 1998, PASP, 110, 79
Fernández, J. A., Licandro, J., Moreno, F., et al. 2017, Icar, 295, 34
Fernández, J. A., & Sosa, A. 2015, P&SS, 118, 14
Fernández, Y. R., McFadden, L. A., Lisse, C. M., Helin, E. F., & Chamberlin, A. B. 1997, Icar, 128, 114
Filacchione, G., Groussin, O., Herny, C., et al. 2019, SSRv, 215, 19
Filippenko, A. V. 1982, PASP, 94, 715
Fink, U., Hoffmann, M., Grundy, W., Hicks, M., & Sears, W. 1992, Icar, 97, 145
Gimeno, G., Roth, K., Chiboucas, K., et al. 2016, Proc. SPIE, 9908, 99082S
Gulbis, A. A. S., Bus, S. J., Elliot, J. L., et al. 2011, PASP, 123, 461
Harris, A. W. 1998, Icar, 131, 291
Harris, C. R., Millman, K. J., van der Walt, S. J., et al. 2020, Natur, 585, 357
Hasegawa, I. 1979, PASJ, 31, 257
Hicks, L. J., MacArthur, J. L., Bridges, J. C., et al. 2017, M&PS, 52, 2075
Hicks, M. D., & Bauer, J. M. 2007, ApJL, 662, L47
Hook, I. M., Jørgensen, I., Allington-Smith, J. R., et al. 2004, PASP, 116, 425
Hsieh, H. H., Novaković, B., Walsh, K. J., & Schörghofer, N. 2020, AJ, 159
Jenniskens, P. 2004, AJ, 127, 3018
Jenniskens, P., Betlem, H., de Lignie, M., Langbroek, M., & van Vliet, M. 1997, A&A, 327, 1242
Jewitt, D., & Li, J. 2010, AJ, 140, 1519
Jewitt, D. C. 2002, AJ, 123, 1039
Jones, G. H., Knight, M. M., Battams, K., et al. 2017, SSRv, 214, 20
Kareta, T., Reddy, V., Hergenrother, C., et al. 2018, AJ, 156, 287
Kasuga, T., & Jewitt, D. 2015, AJ, 150, 152
Kasuga, T., & Jewitt, D. 2019, in Meteoroids: Sources of Meteors on Earth and Beyond, Vol. 8, ed. G. O. Ryabova et al. (Cambridge: Cambridge Univ. Press), 187
Lebedinets, V. N. 1985, AVest, 19, 152
Levison, H. F., Terrell, D., Wiegert, P. A., Dones, L., & Duncan, M. J. 2006, Icar, 182, 161
Licandro, J., Campins, H., Hergenrother, C., & Lara, L. M. 2003, A&A, 398, L45
Luu, J., & Jewitt, D. 1990, Icar, 86, 69
Luu, J. X. 1993, Icar, 104, 138
Marsden, B. G. 2005, ARA&A, 43, 75
McIntosh, B. A. 1990, Icar, 86, 299
Meech, K. J., Hainaut, O. R., & Marsden, B. G. 2004, Icar, 170, 463
Oklay, N., Sunshine, J. M., Pajola, M., et al. 2016, MNRAS, 462, S394
Rayner, J. T., Toomey, D. W., Onaka, P. M., et al. 2003, PASP, 115, 362
Reddy, V., Emery, J. P., Gaffey, M. J., et al. 2009, M&PS, 44, 1917
Reddy, V., Gaffey, M. J., Abell, P. A., & Hardersen, P. S. 2012, Icar, 219, 382
Rein, H., & Liu, S.-F. 2012, A&A, 537, A128
Rein, H., & Spiegel, D. S. 2015, MNRAS, 446, 1424
Rivkin, A. S., Binzel, R. P., & Bus, S. J. 2005, Icar, 175, 175
Ryabova, G. O. 2016, MNRAS, 456, 78
Sekanina, Z., & Chodas, P. W. 2005, ApJS, 161, 551
Tubiana, C., Snodgrass, C., Michelsen, R., et al. 2015, A&A, 584, A97
Virtanen, P., Gommers, R., Oliphant, T. E., et al. 2020, Nature Methods, 17, 261
West, R. M. 1991, A&A, 241, 635
Whipple, F. L. 1983, IAUC, 3881, 1
Wiegert, P., & Brown, P. 2005, Icar, 179, 139
Willmer, C. N. A. 2018, ApJS, 236, 47
Yang, B., & Jewitt, D. 2010, AJ, 140, 692